JOURNAL OF GEOPHYSICAL RESEARCH, VOL. 89, NO. D2, PAGES 2616–2626, APRIL 20, 1984

Correcting Satellite Doppler Data for Tropospheric Effects

H. D. BLACK AND A. EISNER

Applied Physics Laboratory, The Johns Hopkins University

Using a simple geometrical model, and one fitted parameter, tropospheric effects can be effectively removed from satellite Doppler data at microwave frequencies. Both the wet and the dry parts of the tropospheric refraction effect are removed. The technique works best for low (say, 1200 km or less) altitude satellites. For these satellites, the pass (transit) duration limits the required atmospheric correlation time to about 20 min. The effective thickness of the neutral atmosphere (10 km for the wet and 45 km for the dry) limits the required correlation distance to a few degrees in latitude and longitude. These conditions are satisfied often enough to make the fitting technique highly useful. The fitted parameter together with minimal dependence on model structure appears to skirt a difficult problem, modeling the water vapor distribution in a poorly mixed atmosphere. Experimental results (for a limited time period) confirm that the approach is valid on a global basis. In another context, this technique can be used to intensively sample the precipitable water vapor in the atmosphere without using balloons.

1. INTRODUCTION

In correcting satellite Doppler data for the refractive effect of the neutral atmosphere it is necessary to compute the correction to the instantaneous satellite slant range. This is given by the expression

$$\Delta s = 10^{-6} \int N d\rho \tag{1}$$

where N is the refractivity

$$N \triangleq 10^6 (n - 1) \tag{2}$$

and n is the index of refraction. The integral is to be evaluated along an extremum path (connecting the observer and the satellite) consistent with Fermat's principle.

2. INDEX OF REFRACTION

The index of refraction of the troposphere is the sum of two effects [*Smith and Weintraub*, 1953; *Thayer*, 1974], one that depends on water vapor and one that does not. The Smith/Weintraub formula for the atmospheric refractivity is

$$N = N_d + N_w \tag{3}$$

wherein the "dry" term is

$$N_d = 77.6\ P/T \tag{4}$$

and the "wet" term is

$$N_w = 3.73 \times 10^5 (e/T^2) \tag{5}$$

where $N \triangleq 10^6 \times (n - 1)$, the "refractivity"; n = index of refraction; P = total pressure, millibars (1 atm = 1013.25 mbar); T = temperature, Kelvin; e = partial pressure of the water vapor, millibars. (The Smith/Weintraub expression is valid for frequencies less than about 30 GHz.) It is convenient to talk of the dry and the wet effects.

3. DRY TERM

The dry term, 85–90% of the combined tropospheric (range) effect, is highly "predictable" and can be accurately modeled [*Hopfield*, 1971; *Black*, 1978]:

The dry tropospheric range correction, for elevation angles above 10° is given by

$$\Delta s = 2.343\ P_s \left(\frac{T - 4.12}{T}\right) I_d \tag{6}$$

wherein

$$I_d \triangleq \left\{1 - \left[\frac{\cos E}{1 + \chi_c h_d / Re}\right]^2\right\}^{-1/2} \tag{7}$$

χ_c is a weak function of the elevation angle and surface temperature, $\chi_c \to 1/6$ for elevation angles greater than 15°, and if χ_c were 0, then I_d would reduce to csc E; h_d, the "extent" of the dry troposphere, a linear function of surface temperature $35 \leq h_d \leq 45$ km (see eq. (18)); T is the surface temperature in degrees K; P_s is the surface pressure in normal atmospheres; Δs is the tropospheric range effect in meters; E is the instantaneous satellite elevation angle; and R_e is the distance from the earth's center to the observer.

Above 15° elevation angle the important functional dependence, implicit in (6), is embodied in

$$\Delta s = 2.34\ P_s \left[\frac{T - 4.12}{T}\right] \csc E \tag{8}$$

Here we see that the important variables are surface pressure at the observation site and the satellite elevation angle. The temperature dependence (except below 5° elevation angle) is so weak that it is unimportant. The dry effect is 20 m or less for elevation angles greater than 7°. The *Hopfield* [1971] theory on which this analysis is based is good to about 1%; therefore, the residual error is less than 20 cm, provided we have surface pressure measurement at the site that is good to, say, 1 : 1000 or 1 mbar.

4. WET TERM

The wet term is not easily described, but progress has recently been made [*Goldfinger*, 1980]. When Goldfinger's work is combined with that of *Reitan* [1963] we find that the wet term correction is proportional to the "precipitable water vapor" in the atmosphere and that the latter quantity is, on the average, linear in the surface dew point. "On the average" is an important qualifier. It is frequently true that the water vapor is poorly mixed in the atmosphere; consequently, surface measurements do not characterize the water vapor aloft. Reitan averaged readings for a month and found that out of a

Paper number 3D1948.

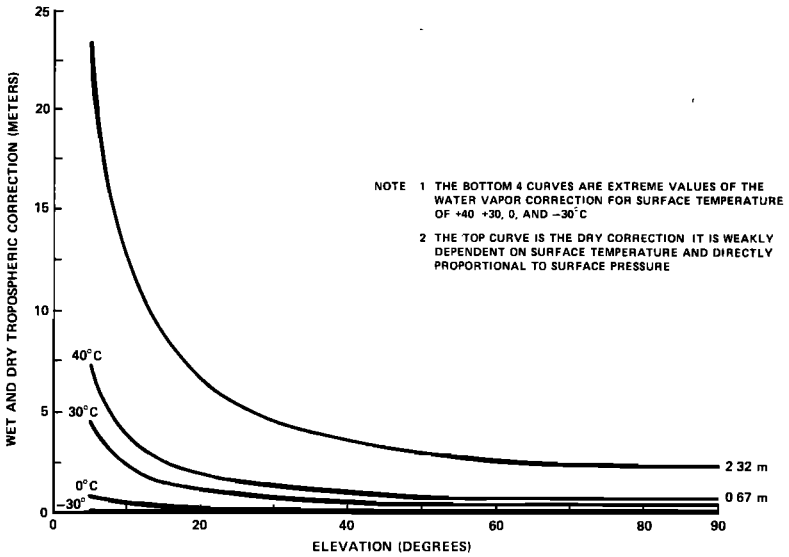

Fig. 1. Wet and dry tropospheric range correction.

total (vertical) correction of 20 cm, the residual error (assuming surface dew point measurements) was about one third of this amount, or 7 cm, and largely random. *Moran and Rosen* [1979] give results that are consistent with these: Along the zenith, they find that surface water vapor density measurements produce the path (range) correction to 5 cm for summer data and 2 cm for winter data. Microwave brightness temperature (radiometer) measurements near 22.235 GHz do about a factor of 5 better [*Guiraud et al.*, 1979]. This is the state of the art.

Some simulated values of the dry and wet range corrections are shown in Figure 1. The dry values are highly precise; the wet values are not. They assume extreme (saturated) conditions at the specified surface temperature and an exponential decrease of water vapor density with height, cf. Figure 2. Typical wet values are one half to one third of those that are shown in Figure 1.

5. The Problem and Its Analysis

This is the 1980 status of WTRVPR measurements/knowledge:

1. *Guiraud et al.* [1979] at NOAA, Boulder, get agreement of 1 cm along the vertical (5.8 cm at 10°) between two-frequency radiometer measurements and radiosonde (balloon) measurements. WTRVPR correction can change a factor of 4 in a few hours. Models utilizing ground measurements agree with two-frequency radiometer measurements (rms) 4 cm along vertical.

2. VLBI, the Aries system at the Jet Propulsion Laboratory (G. Resch, private communication, 1981), currently limits elevations to angles above 20° to minimize propagation errors.

3. G. Resch (private communication, 1981), reports that the WTRVPR correction cannot be correlated with time of day or season.

4. *Hargrave and Shaw* [1978] give a vertical correction for WTRVPR that changes 2 cm in 10 km along the horizontal. Measurements were made in the United Kingdom.

5. *Moran and Rosen* [1979]: rms error of zenith path correction from surface data was 3.2 cm. On the average, scale height of WTRVPR is 2.2 km. See also *Reber and Swope* [1972].

6. *Reitan* [1963] gives the scale height of WTRVPR as 2.2–2.86 km. Monthly means of precipitable WTRVPR correlate well with surface dew point ln $W = a + bt$.

7. *Roosen and Angione* [1977]: Relation between precipitable water vapor and surface humidity shows a strong positive correlation, but the variance is so large that surface humidity is not a reliable indicator of precipitable water vapor for any particular day.

8. *Pitts et al.* [1977] report a case in which the precipitable water vapor changes 1.25 cm over a 3-hour period. The associated horizontal scale is 100 km. (The associated change in vertical range correction is 7.5 cm.)

9. *Goldfinger* [1980] shows that the range correction along the vertical is approximately 6 P_{wv}. The units are the same as

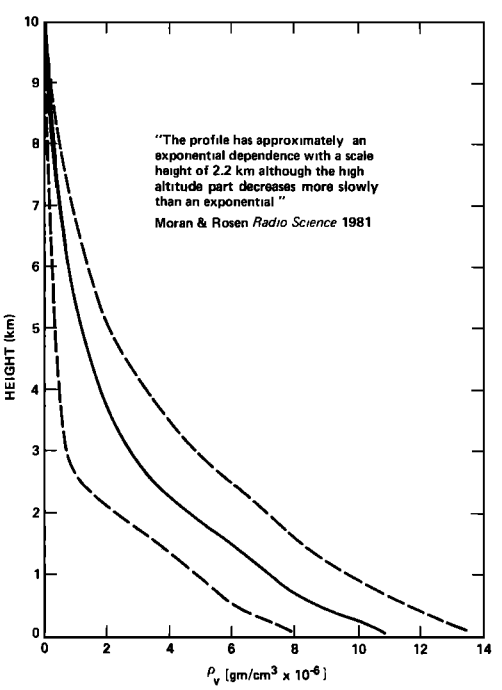

Fig. 2. The mean profile of the water vapor; data from 45 radiosonde launches at Haystack Observatory in August 1975. The dotted lines denote ±1 standard deviation.

those of the precipitable WTRVPR, P_{wv}. *Prabhakara and Dalu* [1980] give synoptic maps of P_{wv} from NIMBUS 4 and NIMBUS 6 data.

We would like to have an expression such as equation (6) for the wet tropospheric range effect which we could use, together with (6) to correct the instantaneous range for both the wet and dry effects. It is clear from the work of Moran and Rosen (and others, see below) that no such expression can be written which is more accurate than about 7 cm along the vertical (60 cm at 7° elevation).

The nonequilibrium and variability of the atmospheric water vapor deny this possibility. Faced with this barrier, we have found that the following approach is a reasonable one.

We can write the sum of the wet and dry corrections:

$$\Delta s = 10^{-6}[\int N_d d\rho + \int N_w d\rho] \tag{9}$$

wherein the refractivities are [*Smith and Weintraub*, 1953] given in (4) and (5) and repeated here

$$N_d = 77.6 \frac{P}{T} \tag{10}$$

$$N_w = (3.73 \times 10^5\ ^\circ\mathrm{K}^2/\mathrm{mbar}) \frac{e}{T^2} \tag{11}$$

(e, T, P) are the water vapor pressure, temperature, and atmospheric pressure. All are point functions of position within the atmosphere. The geometry and associated nomenclature is shown in Figure 3.

For our purposes—as will be seen—the exact form of N_d and N_w are relatively unimportant. We have given (10) and (11) to emphasize that both N_d and N_w are point functions of position within the troposphere. Important for our purposes is the fact that both the dry and wet troposphere extend to heights above the earth's surface that are small compared with the earth's radius; the dry tropospheric effect peters out below $h_d \simeq 45$ km and the wet below $h_w \simeq 13$ km (see *Hopfield* [1971] and Figure 2).

Equation (6) is an evaluation of the first integral of (9) using (10) for the refractivity. In the evaluation, the temperature is assumed to decrease linearly with height, and the atmosphere is assumed to be in hydrostatic equilibrium. (For details see *Black* [1978] and *Hopfield* [1969].)

Before attacking the combined effect we need two facts:

1. *Hopfield* [1976*a*] and others have found from ray-tracing studies that ray bending is unimportant except at low (less than 15°) elevation angles. For relatively high elevation angles, we can use the straight-line path for evaluating the integrals. For elevation angles above 15°, Hopfield's results show that the bending effect is appreciably less than 1 cm. More on this later.

2. *Gardner* [1977] showed that the line-of-sight effect of a horizontal gradient in the (dry) troposphere is typically ½–1 cm (peak value = 1.25 cm) if elevation angles above 20° are utilized. If we include the 10°–20° elevation interval, then the gradient effect increases to 2–3 cm (peak value = 5 cm). Gardner's findings were for the mid-Atlantic seaboard during January–February 1970. See also item 4 in the list concerning the status of WTRVPR measurements/knowledge.

Even though the water vapor is not well mixed in the atmosphere, it is more closely confined to the surface, and the overall effect is 10–15% of the dry effect (integral). We will assume that the gradient effects of the wet troposphere are no greater than those in the dry (i.e., ½–1 cm for all elevation angles above 20°. As a result of these two facts/assumptions we can use a straight-line through the troposphere to evaluate the integral and also ignore gradients.

We can now write (9) as

$$\Delta s = 10^{-6} \int (N_d + N_w)\, d\rho \tag{12}$$

where the integration path is now the straight line (slant range) connecting the observer and satellite (Figure 3).

From the geometry in the sketch we obtain

$$d\rho = \frac{dh}{\{1 - [\cos E/(1 + h/R_e)]^2\}^{1/2}}$$

and (12) can be written

$$\Delta s = 10^{-6} \int_0^{h_d} (N_d + N_w) \frac{dh}{\{1 - [\cos E/(1 + h/R_e)]^2\}^{1/2}} \tag{13}$$

Since $h_d > h_w$ we can write

$$N_w = \begin{cases} 3.73 \times 10^5\, e/T^2 & \text{if } h \le h_w \\ 0 & h_w < h \end{cases} \tag{14}$$

cf. equation (11).

The term h/R_e, in (13), is much less than 1; h_d/R_e is less than 0.007 for the dry term (see equation (18)) and h_w/R_e is less than 0.002 for the wet term (see Figure 2). This suggests that we write (13) as

$$\Delta s = 10^{-6}\, I_{dw} \int_0^{h_d} (N_d + N_w)\, dh \tag{15}$$

wherein

$$I_{dw} = \left\{1 - \left[\frac{\cos E}{1 + \chi_{dw} h_d/R_e}\right]^2\right\}^{-1/2} \tag{16}$$

for some $0 < \chi_{dw} < 1$.

(This is an expansion of the bracketed term in (13) in a series about a point within the troposphere keeping only the zeroth-order term.) I_{dw} is a generalization of the cosecant; if $\chi_{dw} = 0$, then I_{dw} reduces to csc E. As $I_{dw}(E = 90°) = 1$, the integral in (15) is the zenith correction. It is useful to realize the following points:

1. Equation (13), the precise one, and equation (15), the approximate one, approach the same form as the elevation angle approaches 90°.

2. Equation (15) removes the apparent singularity at the lower limit (in equation (13)) when $E = 0$.

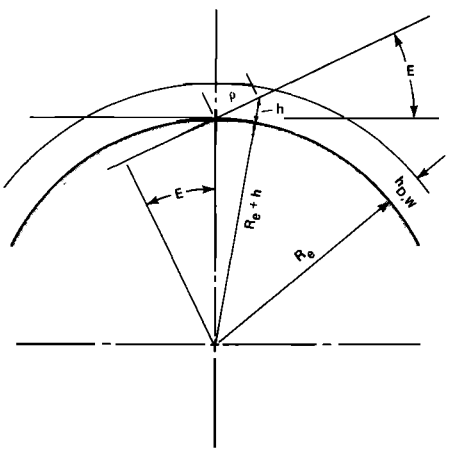

Fig. 3. Tropospheric geometry.

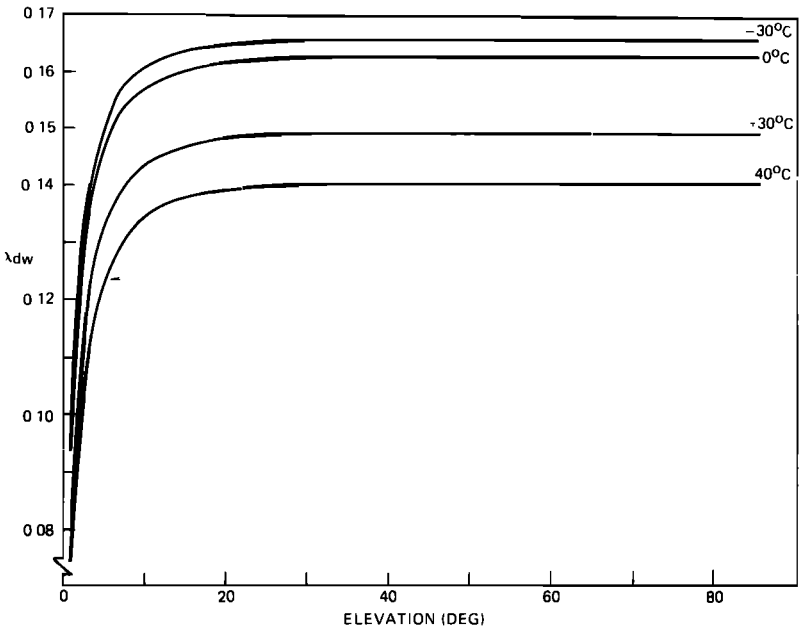

Fig. 4. Dimensionless parameter in model.

3. Since the satellite usually does not pass through the zenith, the integral in (15) is the zenith effect only if the horizontal gradients are negligible. Since the dry effect is proportional to the surface pressure, surface pressure variations from a weather map are a convenient way of evaluating the importance of gradients.

4. Equation (15) is a convenient factorization of the tropospheric range effect into the form

$$\text{(geometry)} \times \text{(amplitude)}$$

moreover, in the amplitude (the integral) we have "buried" the difficult problem of modeling the atmospheric state. This form anticipates our eventual need for a form having a single free quantity which we can, in turn, estimate from the Doppler data. This point will be clarified as the analysis proceeds. A more precise formulation is possible if we admit separate χ values for both the wet and dry parts of the troposphere. Such a form would presuppose that we have an independent technique for determining the amplitude of either the wet or dry term.

Using the above equations we can (by equating the right sides of (13) and (15)) derive the χ_{dw} which makes (15) exact:

$$\chi_{dw} = \frac{R_e}{h_d}\left\{\left[\frac{I_R{}^2}{I_R{}^2 - 1}\right]^{1/2} \cos E - 1\right\} \tag{17}$$

wherein

$$\begin{aligned} h_d &= 148.98\ (T - 4.12)\ \text{m} \\ &= 46.041\ \text{km} \end{aligned} \tag{18}$$

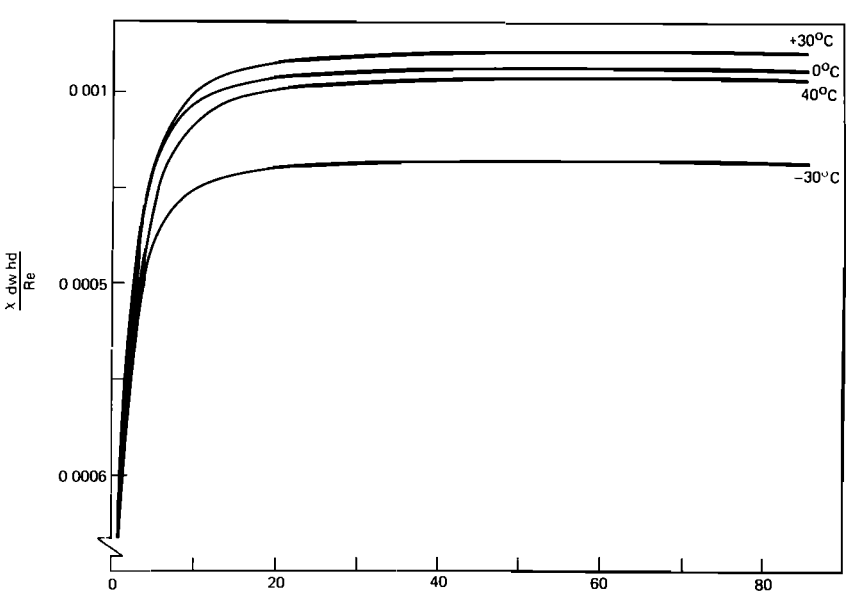

Fig. 5. Dimensionless parameter in equation (16).

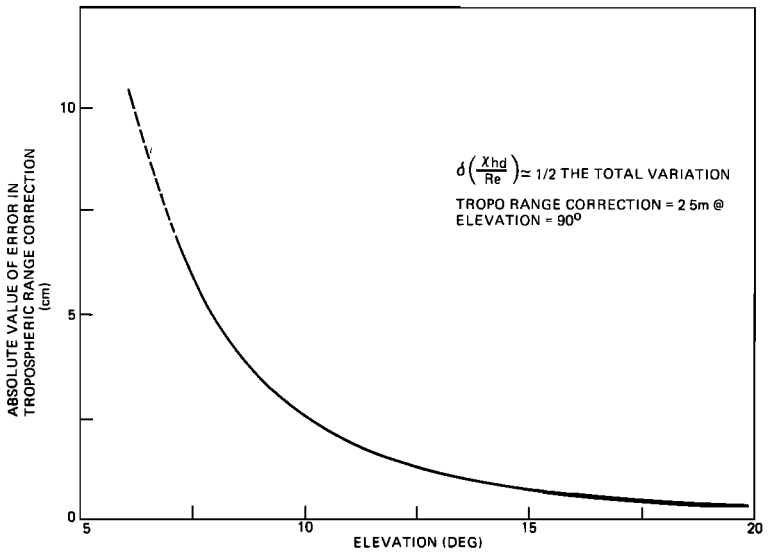

Fig. 6. Approximation error in computing tropospheric range error.

for $T = 313$ K (40°C) [*Hopfield*, 1971] and I_R is the ratio of two integrals

$$I_R = \frac{\int_0^{h_d} (N_d + N_w) \dfrac{dh}{\{1 - [\cos E/(1 + h/R_e)]^2\}^{1/2}}}{\int_0^{h_d} (N_d + N_w)\, dh} \tag{19}$$

Using (17), (18), (19), (4), and (5), numerical integration and representative (modeled) vertical profiles of the temperature and water vapor, we have computed values of dimensionless quantity χ_{dw}. For the temperature-height distribution, we used a constant lapse rate, and for the water vapor an exponential height profile with saturated conditions at the surface. Results are shown in Figure 4 for surface temperatures of −30°, 0, +30°, and 40°C. From the figure it is clear that χ_{dw} is a constant (here, because of the way we parameterized the water vapor distribution, characterized by the surface temperature) for all elevation angles exceeding 15°. For this elevation interval $0.141 \leq \chi_{dw} \leq 0.16\underline{6}$. These are the extreme values for all conditions: The vapor pressure is so low at −30°C that the saturated vapor pressure contributes negligibly to the upper bound on χ_{dw}. We showed [*Black*, 1978] that $\chi_{dw}(E = 90°) = 0.16\underline{6}$ for the dry effect alone for all temperatures. It seems reasonable to conjecture that the above extreme values are extremes over most (all?) water vapor profiles.

Since the dimensionless combination $\chi_{dw}(h_d/R_e)$ appears in (16) (h_d given by equation (18)) we have plotted this quantity in Figure 5. Between 7° and 90° elevation and for surface temperatures between −30°C and +40°C the variation in this quantity is

$$0.00088 \leq \left(\frac{\chi_{dw} h_d}{R_e}\right) \leq 0.0010$$

(a tedious computation shows that the upper bound is given by $1/6\ h_d/R_e$) or to three significant digits

$$\frac{\chi_{dw} h_d}{R_e} = 0.001$$

We will tentatively accept that (see (15) and (16))

$$\Delta s = \left[10^{-6} \int_0^{h_d} (N_d + N_w)\, dh\right] I_{dw} \tag{20}$$

wherein

$$I_{dw} = \left[1 - \left(\frac{\cos E}{1 + 0.001}\right)^2\right]^{-1/2} \tag{21}$$

for elevations between 7° and 90° and for surface temperatures between −30°C and +40° C. Equations (20) and (21) are certainly precise enough to use for an error analysis: Figure 6 shows the error in the tropospheric range correction caused by an error in $(\chi_{dw} \cdot h_d/R_e)$ equal to one half of the variation; $\frac{1}{2}(1-0.88) \times 10^{-3} = 0.06 \times 10^{-3}$. The error is about 7 cm at 7° elevation; much less than 1% of the correction itself. This is a bound on the error for higher elevation angles, as is seen from Figure 6: Above 13° the error in this formalism is less than 1 cm. The associated error in range difference, subsequently required in a surveying computation, will be less than this; the mean value of the "formal" error, since it is highly correlated over the differencing interval, will subtract out.

6. Bending Effect

To this point, we have given the bending effect, of some concern at very low elevation angles, only cursory attention. We do not intend to treat this subject in any depth.

Hopfield [1976*b*] comments that ". . . Although the geometrical path is greater than the slant range between two points, the electromagnetic range is less along the curved path than along the slant-range vector." She includes the following (Table 1) model for the bending effect, and she includes it in her 1976 report [see also *Hopfield*, 1979]. We have not used it here; but, note the following.

We have computed values of the tropospheric range correction by numerically integrating (13) (neglecting bending) and have compared the correction with the approximate values given by (20) and (21). The precise values are given in Table 2. The differences (approximate minus precise) are given in parenthesis above the corresponding precise values. As is clear, the error in the approximate form partially compensates for the bending effect. The compensation is not as good as we would like (cf. Table 1). Nevertheless, it is of some benefit. Clearly, the way to deal with the bending effect is to use the Hopfield model to correct the data and simultaneously use a table to remove the errors (at low elevation angles) in (21). For

TABLE 1. Effect of Bending

Elevation, deg.	Δ_s (Bending), m	$\sigma(\Delta s_b)$, m
1	3.11	0.19
5	0.19	0.006
10	0.03	0.0009

elevation angles below 5° there is another problem as the elevation angle approaches zero: The dry part becomes increasingly more sensitive to variations is temperature lapse rate [*Black*, 1978; *Maejima*, 1977].

7. Fitting Procedure

We intend to use (20) and (21) to model the tropospheric range effect Δs. All of the geometrical dependence is contained in I_{d_w}. We will consider the integral (the zenith correction)

$$\Delta s_z = 10^{-6} \int_0^{h_d} (N_d + N_w)\, dh \tag{22}$$

as a to-be-determined quantity associated with each 15-min pass of satellite data. We will use the model, from this point on, as

$$\Delta s = \Delta s_z \left[1 - \left(\frac{\cos E}{1 + 0.001} \right)^2 \right]^{-1/2} \tag{23}$$

The instantaneous slant-range to the satellite is written at the ith time point

$$\rho_i = \left| \bar{r}_s \left(t_i - \frac{\rho_i}{c} \right) - \bar{r}_N(t_i) \right| + \Delta s_i^{\text{TRO}} + \Delta s_i^{\text{REL}} \tag{24}$$

wherein $\bar{r}_s$ is the position of the satellite; $\bar{r}_N$ is the position of the observer; Δs_i^{REL} is the relativistic correction to the slant-range; Δs_i^{TRO} is the tropospheric correction to the slant-range (equation 23); t_i time on the ground of the ith measurement; and c is the speed of light.

This question immediately arises: Is it possible, without constraints, to determine a parameter in addition to the three (along-track and slant range at closest approach plus frequency bias) that are already being determined? We answer this question as follows.

TABLE 2. Precise Values

	Elevation			
	−30°	0°	+30°	+40°
5.2	(−35.7)	(−17.4)	(−18.4)	(−29.7)
	23.411	23.923	27.330	30.014
6.4	(−17.5)	(−6.2)	(−5.4)	(−10.7)
	19.473	19.941	22.777	24.989
7.0	(−12.8)	(−3.8)	(−2.6)	(−6.5)
	17.908	18.354	20.963	22.991
10.4	(−3.4)	(−0.1)	(+0.9)	(−0.1)
	12.524	12.867	14.698	16.105
11.8	(−2.2)	(+0.1)	(+1.0)	(+0.4)
	11.091	11.402	13.024	14.268
14.8	(−1.1)	(+0.2)	(+0.8)	(+0.6)
	8.929	9.185	10.493	11.493
17.3	(−0.6)	(+0.2)	(+0.7)	(+0.5)
	7.726	7.951	9.084	9.948

Errors in approximate form, in centimeters, otherwise in meters. Values in parenthesis are in centimeters. Values not in parenthesis are in meters.

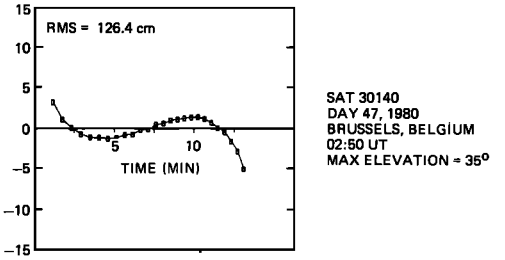

Fig. 7. Tropospheric signal remaining in Doppler residuals after three parameters are fitted out.

Figure 7 shows the after-fit residuals from a pass of data. (The tropospheric model was omitted in the processing.) Three parameters were determined. We compare this figure with a simulation based on (23) (the best fitting straight line was removed from the latter). Results are shown in Figure 8. Clearly, there is a tropospheric signal in the data residuals. The low elevation data is crucial in separating the tropospheric amplitude from the other data biases; the maximum elevation of the pass should exceed (approximately) 20° (see Figure 1) for the tropospheric signal to be fully represented in the Doppler data.

8. Horizontal Correlation Length

To make the fitting process tractable, we ignore horizontal gradients (in the wet and dry refractivity) within the troposphere. In other words, we are assuming that the troposphere is horizontally stratified. This, in turn, imposes the constraints that the surface pressure and the precipitable water vapor

$$p_{wv} = \frac{1}{\rho_w} \int \rho_{wv}\, dh$$

where ρ_w is the density of liquid water, in the neighborhood of the observing site be constant. Over the time duration of a satellite transit, we are also assuming that the troposphere does not change; in particular, that Δs_z remains constant. Since we are utilizing a satellite with a (nominal) altitude of 1100 km, the transit duration is less than 20 min. Moreover, since the thickness of the troposphere is small compared with the radius of the earth, the "constant" neighborhood is spatially limited. Figures 9 and 10 illustrate this limitation. The neighborhood for the dry troposphere need not extend more than 300 km around the observing site if we use data no lower than 7.5° in elevation. The corresponding neighborhood for

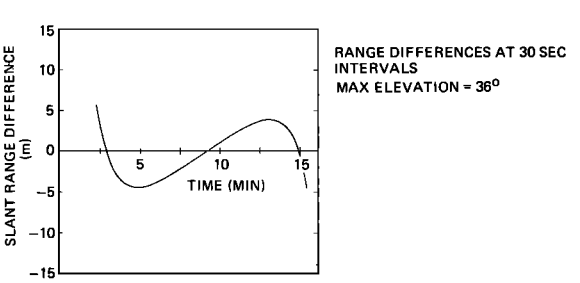

Fig. 8. Simulated tropospheric range-difference error.

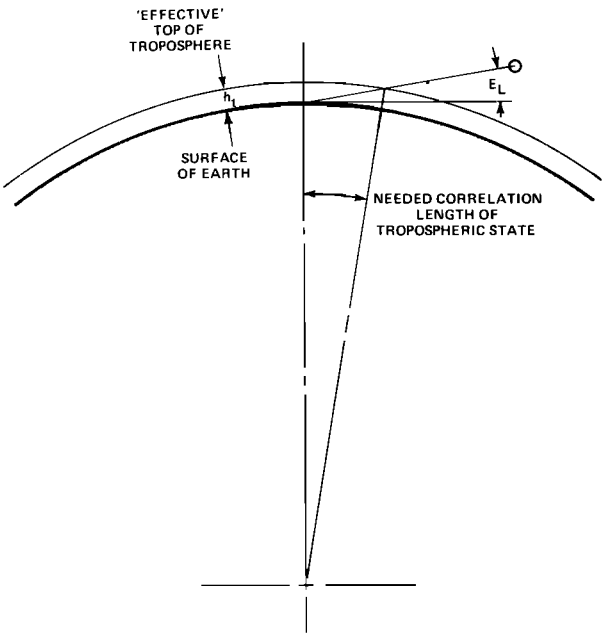

Fig. 9. Tropospheric geometry and needed correlation length.

the wet term is 130 km in radius. A glance at several weather maps indicates that the along-the-surface pressure variation does not appreciably affect the dry term.

9. Experimental Results

The Doppler data we used were characterized as follows: (1) obtained at a globally distributed set of sites; (2) two of the five Transit satellites 30140 and 30480 were utilized; (3) one 2-day data span was obtained during winter in the northern hemisphere, February 1980 (days 48–49) and another during summer July 1982 (days 197–198); (4) each data span contained approximately 80 passes. Using each data span (and the Hopfield model) we determined an ephemeris for the satellite. Subsequently, we used the ephemeris and processed the individual passes two different ways:

1. The tropospheric model was again used (the tropospheric parameter was not estimated) and the remaining pass-associated biases were absorbed in three least squares determined parameters; two components of the station position, the "along-track" parameter, and the slant-range parameter. These two quantities associate data biases, from whatever source, with the station position. The third parameter is the frequency bias between the satellite and ground oscillator.

2. The model, equation (23), was included, and the amplitude, Δs_z, was least squares fitted together with the other three parameters (see above). No a priori constraints were used.

Figure 11 shows the individual Δs_z values,

$$\Delta s_z = 10^{-6} \int_0^{h_d} (N_d + N_w)\, dh$$

for days 198–199. Since the dry term dominates (and lower bounds) this integral and it is, in turn, proportional to the surface pressure at the ground sites, we have plotted Δs_z versus the surface pressure. The straight line is the dry term; 2.305 P_s, with an associated uncertainty of 1–2%, about 3 cm. Since the dry term provides a lower bound on the tropospheric range correction and wet values above 60 cm are unrealistic, there are four "wild" data points. After removing these points, the mean values at each site were computed. These mean values for both data sets are shown in Figure 12. Four stations were represented in both data sets; Johannesburg, South Africa; Las Cruces, New Mexico; San Jose Dos Campos, Brazil; and Herndon, Virginia. The data at these four sites agree with the (usually true) finding that the atmosphere contains more water vapor in the summer than it does in the winter. A tabulation of the results shown in Figure 12 is given in Table 3.

If we fit the tropospheric parameter rather than using a model per se, as indicated above, station position differences are a result. These differences are shown in Figure 13 (1982 data) and indicate that there are important considerations here in correcting for tropospheric effects in satellite-derived surveying computations. As Figure 13 shows most of the tropospheric bias will appear in the slant-range coordinate which will in turn bias the longitude and station height. There are, however, along-track (latitude) effects as well.

10. Discussion

We believe that Figures 11 and 12 verify that this simple geometrical technique works and, moreover, is a convenient and accurate one to use when surface meteorological data is not available and perhaps when it is available.

We have not as yet answered an important question: Is tropospheric fitting really better than utilizing a model per se? An indication from this study is that it should be. Wet-term models cannot be made very precise, and, moreover, it is certainly convenient to avoid dealing with meteorological data.

To show whether or not the fitted parameter gives higher accuracy in station position determination, we should repeat the experiment carried out by *Jenkins et al.* [1979]. At each of several sites we should (1) acquire several (say, 6–10) sets of passes, (2) execute a multi-set survey at each site, and (3) compare the uncertainty of the site coordinates determined with tropospheric fitting and with the model utilizing an a priori–computed amplitude.

Jenkins et al. recognized that there are problems with fitting a tropospheric parameter if there are errors in the satellite ephemeris. We were careful here to assure that the ephemeris, the station coordinates used in deriving the ephemeris, the geopotential model, and the associated software were all as internally consistent as we could make them.

We had expected to see some evidence of the third-order

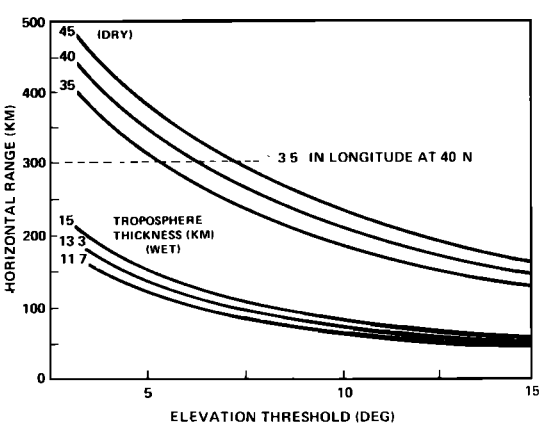

Fig. 10. Upper bound on necessary tropospheric correlation distance.

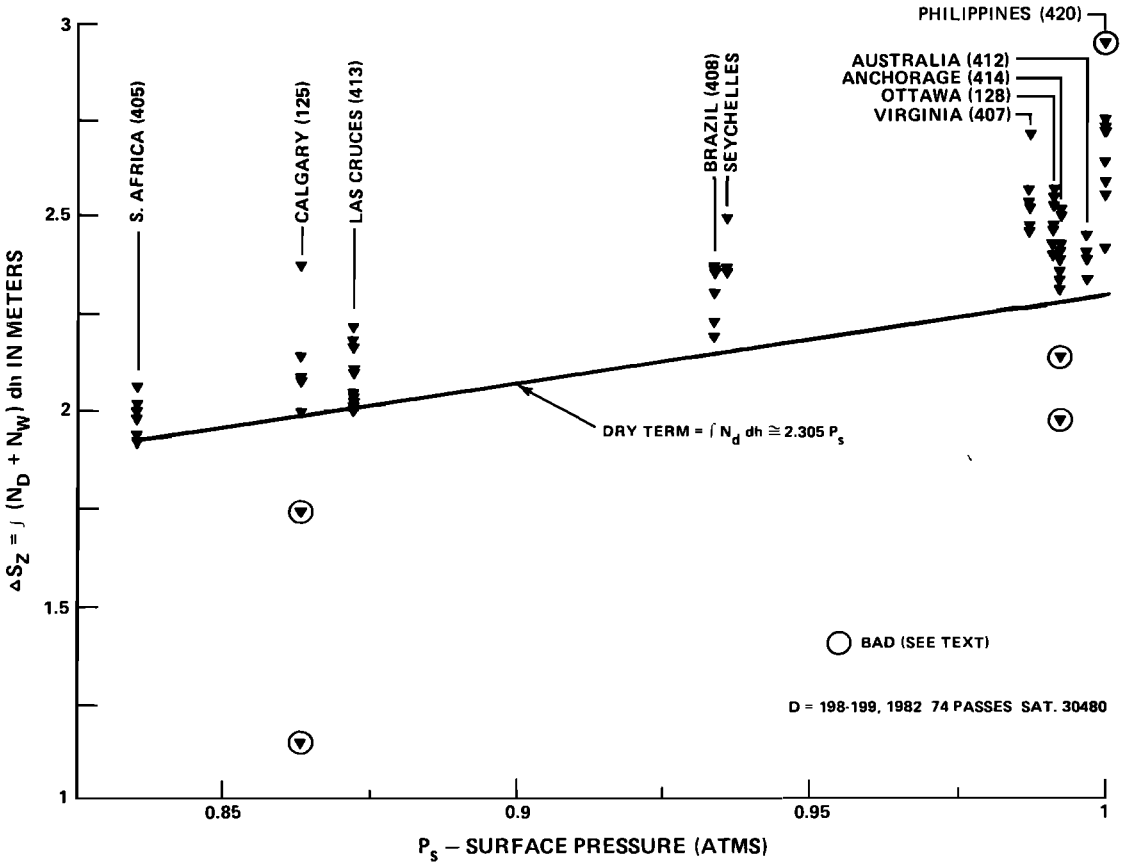

Fig. 11. Fitted tropospheric amplitude.

ionospheric effects in the residuals and results. Except possibly in the Hawaii residuals, we did not see these effects; however, this subject deserves more and extended study.

We have emphasized the use of this technique for removing tropospheric effects from the Doppler data. The results may have value in another context: Since we seem to be determining realistic values of the wet term which can be interpreted as precipitable water vapor [*Goldfinger*, 1980], we possibly have a new technique for intensively sampling (20 times/day) the atmospheric water vapor at the particular site. A surface pressure measurement is required in the data reduction to remove the dry term. A 2.4-cm error incurred in removing the dry term will result in 0.4 cm error in the precipitable water vapor. This appears to be practically achievable.

Before we could decide whether or not the technique is useful and complements other (existing) techniques, further ex-

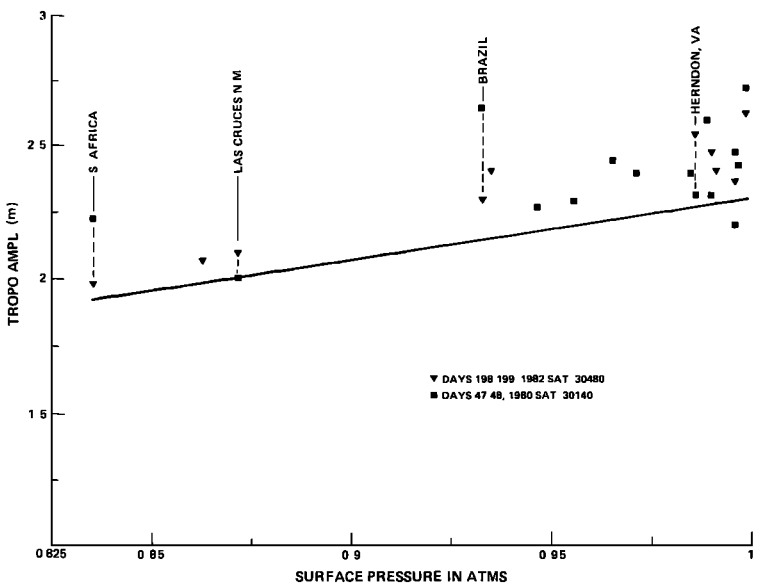

Fig. 12. Pass-averaged values of the tropospheric amplitude.

TABLE 3. Troposphere Fitting Results

	Station	Latitude, deg.	Altitude, m	SAT 30140 Fitted Tropo, $D = 47$–48 1980, m	SAT 30140 Number of Passes	SAT 30480 Fitted Tropo $D = 198$–199 1982, m	SAT 30480 Number of Passes
414	Anchorage, Al.	+61°	69			2.34 ± 0.16*	11
125	Calgary, Canada	+51°	1272			1.95 ± 0.37*	8
021	Brussels, Belgium	+51°	116	2.40 ± 0.40†	7		
128	Ottawa, Canada	+45°	86			2.47 ± 0.06*	9
320	Minnesota	+45°	300	2.45 ± 0.15†	5		
641	Florence, Italy	+44°	100	2.60 ± 0.33†	6		
313	Maine	+44°	24.7	2.43 ± 0.12†	6		
407	Herndon, Va.	+39°	119	2.32 ± 0.12†	8	2.54 ± 0.09*	6
027	Japan	+39°	83	2.32 ± 0.33†	7		
330	California	+34°	462	2.27 ± 0.18†	5		
113	New Mexico	+32°	1206	2.00 ± 0.22†	5		
413	New Mexico	+32°	1206			2.10 ± 0.08*	8
192	Austin, Texas	+30°	245	2.40 ± 0.30†	6		
341	Hawaii	+21°	401	2.29 ± 0.24†	4		
422	San Miguel, P.I.	+15°	12			2.67 ± 0.16*	8
023	Guam	+13°	38	2.48 ± 0.07†	5		
420	Seychelles Island	−4°	593			2.55 ± 0.29†	4
424	American Samoa	−14°	12	2.73 ± 0.17*	4		
008	Brazil	−23°	613	2.65 ± 0.23*	3		
408	Brazil	−23°	613			2.30 ± 0.08†	6
105	South Africa	−26°	1581	2.23 ± 0.21*	7		
405	South Africa	−26°	1581			1.98 ± 0.05†	7
412	Smithfield, Australia	−34°	34			2.37 ± 0.05†	8
019	Antarctica	−78°	38	2.21 ± 0.31*	6		
Total				2.39 ± 0.23	84	2.33 ± 0.23	75

*Summer.
†Winter.

perimentation is required. Certainly, comparison of results with balloon (radiosonde) or radiometer data is called for. The noise on the in-orbit oscillators or the third-order ionospheric errors are possibly limiting the current accuracy of our results. We just do not know.

The reader is perhaps confused over the use of data acquired at low-elevation angles. The issue is far from clear. On the one hand, low elevation data are necessary to separate the refractivity amplitude (Δs_z, equation (22)) from the other necessary, estimated quantities, necessary to absorb orbit and station position errors. On the other hand, as we reduce the elevation angle appreciably below 10°, the errors in the model and, consequently, the correlated errors in the residuals, increase. Our current feeling, based on the noise level of the available data, is that the lowest elevation we can use is 5–7°. Fitting the curves shown in Figure 5 and subsequently using the results as part of the model should slightly improve the model at low elevation angles. To take advantage of this im-

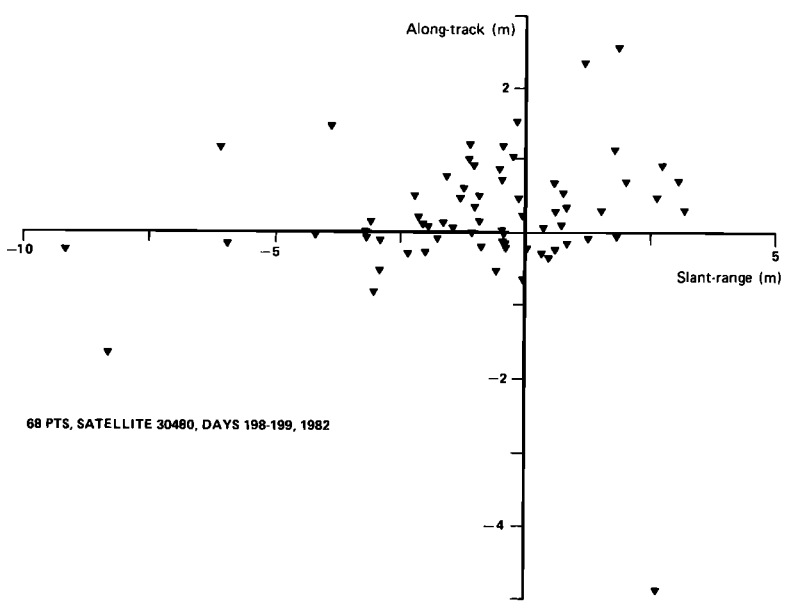

Fig. 13. Station position changes associated with the fitting the tropospheric parameter.

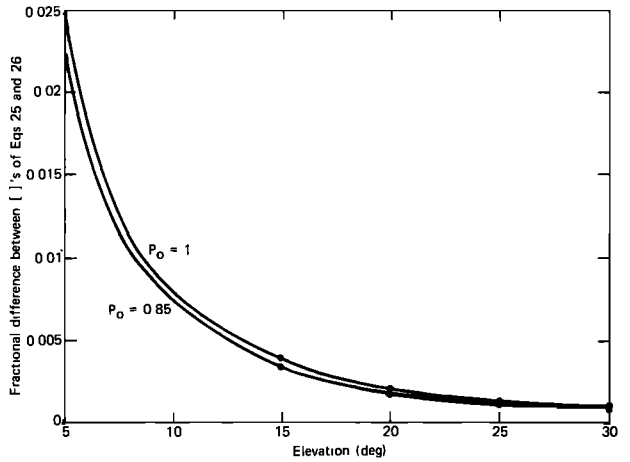

Fig. 14. Normalized differences between the Marini-Murray and Black-Hopfield models.

provement would, however, require on-site temperature and humidity measurements. Expanding (13) to higher orders in h/R_e does not seem like a very promising approach, nor does trying to use data below 5°, because of the sensitivity to temperature lapse rate. If the data quality should improve clearly we should shift to higher elevation cut-off thresholds, consistent with accuracy requirements.

11. Comparison With Other Models

One of the better known models of the tropospheric range effect is that of *Marini and Murray* [1973]. Their work is designed to correct laser data; however, there are enough similarities between the dry tropospheric effect at microwave frequencies and at optical frequencies to make a useful comparison: We ignore the effects of water vapor; the water vapor refractivity at laser wavelengths is 11.26 e/T, whereas at microwave it is (equation (5)) $3.73 \times 10^5\ e/T^2$.

For elevation angles above 5° and for all atmospheric conditions and station heights we can replace their equation (18) with

$$\Delta R = \frac{f(\lambda)}{f(\phi, H)} A\left[\frac{1 + (B/A/(1 + 0.01))}{\sin E + (B/A/(\sin E + 0.01))}\right] \quad (25)$$

The difference between this form and theirs is at most $1.3 \times 10^{-5}\Delta R$.

The term in square brackets is unity for $E = 90°$. The term in front, the amplitude, is (in meters)

$$\frac{f(\lambda)}{f(\phi, H)} A \equiv \frac{2.305\ P_0}{1 - 2.6 \times 10^{-3} \cos 2\phi - 3.1 \times 10^{-4} H}$$

where P_0 is the surface pressure in normal atmospheres, H is the station altitude in kilometers, and ϕ is the station latitude.

From [*Black*, 1978, p. 1828] we obtain a form comparable to (25).

$$\Delta R = 2.343\ P_0\left(\frac{T - 4.12}{T}\right)\left[1 - \left(\frac{\cos E}{1 + 0.16 h_d/r_s}\right)^2\right]^{-1/2} \quad (26)$$

Once again, the term in square brackets has magnitude unity for $E = 90°$. The amplitude, the coefficient in front of the bracket, increases from 2.302 P_0 to 2.312 P_0 as the surface temperature increases from −40°C to +40°C (cf. the Marini-Murray value of 2.305 P_0 for $\phi = 45°$, $H = 0$, and 2.311 P_0 for $\phi = 0°$, $H = 0$). The bracketed terms in (25) and (26) do not superficially resemble each other, but in fact they are quite close together. We computed the fractional difference between the two brackets for $0.85 \le P_0 \le 1$ for elevation angles above 5°, and for $T = 233$, 288; and 313 K. The brackets differ 2.5% at 5° elevation and 0.5% or less for elevations above 10°. The largest fractional difference among these cases is shown in Figure 14. Above 30°, neither bracket differs more than 0.5% from the cosecant of the elevation angle.

We are not the first to estimate a tropospheric zenith parameter. *Herring et al.* [1981] mention that they include the zenith tropospheric delay as a parameter and that "estimates for the propagation delay through the atmosphere and ionosphere in the zenith direction ranged from 6.7 ns (NRAO) to 8.2 ns (Onsala)."

12. A Possible Application

The motivation for solving this problem came out of our successful attempt to design a satellite system to monitor strain in the earth's crust [*Westerfield and Potocki*, 1982]. So that the system would be all-weather and so that it could simultaneously position a large number of sites, we elected to use microwave frequencies. This choice aggravates the tropospheric refraction errors, particularly the water vapor problem; effects at microwave frequencies are about 100 times larger than they are at optical wavelengths.

We can deal with all the other error sources in the system:

1. Ionospheric refraction can be eliminated by utilizing a pair of frequencies in the neighborhood of 400–1200 MHz.
2. Satellite position errors can be effectively removed by simultaneously observing the satellite at several terrestrial points. The points are separated by small distances, small when compared with the satellite altitude. This correlates the satellite errors in determining the relative position of neighboring points.
3. Errors associated with oscillator noise are suppressed by using closed-loop Doppler links.

These three techniques will push their associated errors down to the centimeter level.

Tropospheric refraction is another story. The troposphere is not dispersive; consequently, using multiple frequencies will not help. The refractivity at a point within the troposphere depends on the atmospheric state and temperature, pressure, and water vapor density.

We believe that the approach described in the body of this report either solves or potentially solves this problem.

Acknowledgments. We appreciated the efforts of Carolyn Leroy of the Defense Mapping Agency/Hydrographic Topographic Center in making Doppler data available to us. We acknowledge the contribution of George C. Weiffenbach. He insisted against our objections that something could be done about this problem. This work was supported by the U.S. Department of the Navy, Task Y related to Task S, under contract N00024-83-C-5501.

References

Black, H. D., An easily implemented algorithm for the tropospheric range correction, *J. Geophy. Res.*, *83*, 1825–1828, 1978.

Gardner, C. S., Effects of horizontal refractivity gradients on the accuracy of laser ranging to satellites, *Radio Sci.*, *11*, 1037–1044, 1976.

Gardner, C. S., Correction of laser tracking data for the effects of horizontal refractivity gradients, *Appl. Opt.*, *16*, 2427–2432, 1977.

Goldfinger, A. D., Refraction of microwave signals by water vapor, *J. Geophys. Res.*, *85*, 4904–4912, 1980.

Guiraud, F. O., et al., A dual-channel microwave radiometer for measurement of precipitable water vapor and liquid, *IEEE Trans. Geosci. Electron.*, *GE-17*, 129–136, 1979.

Hargrave, P. J., and L. J. Shaw, Large-scale tropospheric irregularities and their effect on radio astronomical seeing, *Mon. Not. R. Astron. Soc.*, *182*, 233–239, 1978.

Herring, T. A., et al., Geodesy by radio interferometry: Intercontinental distance determinations with sub-decimeter precision, *J. Geophys. Res.*, *86*, 1647–1651, 1981.

Hopfield, H. S., Two quartic tropospheric refractivity profile for correcting satellite data, *J. Geophys. Res.*, *74*, 4487–4499, 1969.

Hopfield, H. S., Tropospheric effect on electromagnetically measured range: Prediction from surface weather data, *Radio Sci.*, *6*, 357–367, 1971.

Hopfield, H. S., Tropospheric effects on signals at very low elevation angles, *APL/JHU Rep. TG 1291*, Johns Hopkins Univ. Appl. Phys. Lab., Laurel, Md., 1976*a*.

Hopfield, H. S., Tropospheric effects on low-elevation angle signals: Further studies, *APL/JHU Rep. SDO 4588*, Johns Hopkins Univ. Appl. Phys. Lab., Laurel, Md., 1976*b*.

Hopfield, H. S., Improvements in the tropospheric refraction correction for range measurement, *Phil. Trans. R. Soc. London Ser. A*, *294*, 341–352, 1979.

Jenkins, R. E., B. D. Merritt, D. R. Messent, and J. R. Lucas, Refinement of positioning software (Doppler), in *Proceedings of the Second International Geodetic Symposium on Satellite Doppler Positioning*, vol. 1, pp. 233–266, University of Texas, Austin, 1979.

Maejima, I., Global pattern of temperature lapse rate in the lower troposphere with special reference to the altitude of snow line, *Geograph. Rep. Tokyo Metro. Univ.*, no. 12, 1977.

Marini, J. W., and C. W. Murray, Correction of laser range tracking data for atmospheric refraction at elevations above 10 degrees, *NASA/GSFC X-591-73-351*, 1973.

Moran, J. M., and B. R. Rosen, The estimation of the propagation delay through the troposphere from microwave radiometer data, in Radio Interferometry Techniques for Geodesy, *NASA Conf. Publ. 2115*, pp. 363–376, 1979.

Pitts, D. E., et al., Temporal variations in atmospheric water vapor and aerosol optical depth determined by remote sensing, *J. Appl. Meterol.*, *16*, 1312–1321, 1977.

Prabhakara, C., and G. Dalu, Passive remote sensing of the water vapor in the troposphere and its meterological significance, in *Atmospheric Water Vapor*, pp. 355–374, edited by A. Deepak et al., Academic, New York, 1980.

Reber, E. E., and J. R. Swope, On the correlation of the total precipitable water in a vertical column and absolute humidity at the surface, *Rep. TR 0172 (2230-20)13*, Aerospace Corp., Los Angeles, Calif., 1972.

Reitan, C. H., Surface dew point and water vapor aloft, *J. Appl. Meterol.*, *2*, 776–779, 1963.

Roosen, R. G., and R. J. Angione, Variations in atmospheric water vapor: Baseline results from Smithsonian observations, *Publ. Astron. Soc. Pacific*, *89*, 814–822, 1977.

Smith, E. K., Jr., and S. Weintraub, The constants in the equation for atmospheric refraction index at radio frequencies, *Proc. of the I.R.E.*, *41*, 1635–1637, 1953.

Thayer, G. D., An improved equation for the radio refractive index of air, *Radio Sci*, *9*, 803–807, 1974.

Westerfield, E. E., and K. A. Potocki, The fault zone monitoring system, paper presented at *Proceedings of the Third International Geodetic Symposium on Satellite Doppler Positioning*, Las Cruces, N. M., February 1982.

H. D. Black and A. Eisner, Applied Physics Laboratory, The Johns Hopkins University, Johns Hopkins Road, Laurel, MD 20707.

(Received May 16, 1983;
revised December 8, 1983;
accepted December 12, 1983.)